Loss of mitochondrial complex I activity potentiates dopamine neuron death induced by microtubule dysfunction in a Parkinson's disease model

Won-Seok Choi,[1,2] Richard D. Palmiter,[3] and Zhengui Xia[1,2]

[1]Department of Environmental and Occupational Health Sciences, Graduate Program in Neurobiology and Behavior, [2]Institute for Stem Cell and Regenerative Medicine, and [3]Howard Hughes Medical Institute, Department of Biochemistry, University of Washington, Seattle, WA 98195

Mitochondrial complex I dysfunction is regarded as underlying dopamine neuron death in Parkinson's disease models. However, inactivation of the *Ndufs4* gene, which compromises complex I activity, does not affect the survival of dopamine neurons in culture or in the substantia nigra pars compacta of 5-wk-old mice. Treatment with piericidin A, a complex I inhibitor, does not induce selective dopamine neuron death in either *Ndufs4*$^{+/+}$ or *Ndufs4*$^{-/-}$ mesencephalic cultures. In contrast, rotenone, another complex I inhibitor, causes selective toxicity to dopamine neurons, and *Ndufs4* inactivation potentiates this toxicity. We identify microtubule depolymerization and the accumulation of cytosolic dopamine and reactive oxygen species as alternative mechanisms underlying rotenone-induced dopamine neuron death. Enhanced rotenone toxicity to dopamine neurons from *Ndufs4* knockout mice may involve enhanced dopamine synthesis caused by the accumulation of nicotinamide adenine dinucleotide reduced. Our results suggest that the combination of disrupting microtubule dynamics and inhibiting complex I, either by mutations or exposure to toxicants, may be a risk factor for Parkinson's disease.

Introduction

Parkinson's disease is a common aging-related neurodegenerative disorder, which is characterized by the selective loss of dopamine neurons in the substantia nigra pars compacta (SNpc) of the brain. Despite intense research, mechanisms underlying selective dopamine neuron death are not well defined. Inhibition of mitochondrial complex I has long been one of the leading theories (Abou-Sleiman et al., 2006). The observation that drug abusers accidentally exposed to 1-methyl-4-phenyl-1,2,3,6-tetrahydropyridine (MPTP) developed Parkinsonism provided the first evidence for this hypothesis because 1-methyl-4-phenylpyridinium (MPP^+), the toxic metabolite of MPTP, is a mitochondrial complex I inhibitor (Langston et al., 1983; Dauer and Przedborski, 2003). Furthermore, complex I activity is decreased in the substantia nigra, skeletal muscle, and platelets of patients with Parkinson's disease (Mizuno et al., 1989; Parker et al., 1989; Schapira et al., 1989). A recent study suggests that some of the subunits of complex I in human Parkinson's disease brains are oxidatively damaged, resulting in the misassembling and functional impairment of complex I (Keeney et al., 2006).

Chronic treatment of rats and mice with rotenone, a well-established complex I inhibitor, induces many key features of Parkinson's disease (Betarbet et al., 2000; Sherer et al., 2003b; Inden et al., 2007; Pan-Montojo et al., 2010). These findings provide further support for the mitochondrial complex I inhibition hypothesis. Ectopic expression of the *Ndi1* gene, a rotenone- and MPP^+-insensitive single-subunit NADH dehydrogenase from *Saccharomyces cerevisiae*, protects dopamine neurons against MPTP and rotenone toxicities in vitro and in vivo, leading to the conclusion that complex I inhibition is obligatory for dopamine neuron death in the rotenone and MPTP models of Parkinson's disease (Sherer et al., 2003a, 2007; Seo et al., 2006; Richardson et al., 2007; Marella et al., 2008).

To examine the concept that complex I inhibition underlies dopamine neuron degeneration, we studied a mouse strain lacking a functional *Ndufs4* gene that encodes one of the 46

Correspondence to Zhengui Xia: zxia@u.washington.edu

Abbreviation used in this paper: AAV, adeno-associated virus; DIV, day in vitro; GABA, γ-aminobutyric acid; MPP^+, 1-methyl-4-phenylpyridinium; MPTP, 1-methyl-4-phenyl-1,2,3,6-tetrahydropyridine; ROS, reactive oxygen species; SNpc, substantia nigra pars compacta; TH, tyrosine hydroxylase.

The Rockefeller University Press $30.00
J. Cell Biol. Vol. 192 No. 5 873–882
www.jcb.org/cgi/doi/10.1083/jcb.201009132

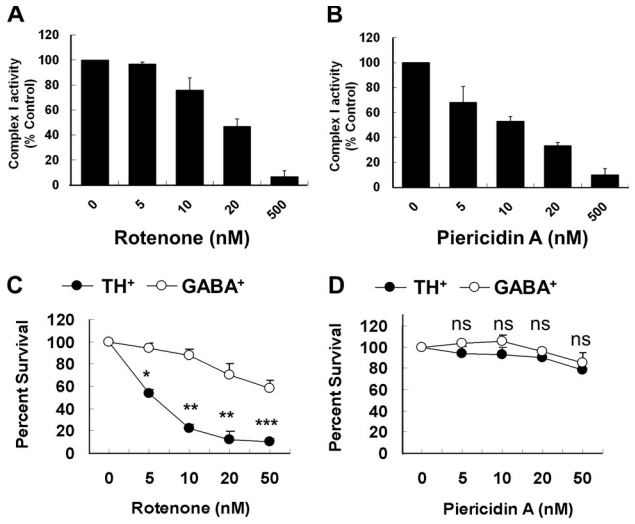

Figure 1. **Complex I inhibition is not sufficient to induce dopamine neuron death.** Primary mesencephalic neurons were cultured from E14 mouse embryos and treated with rotenone or piericidin A after 5 DIV culture. (A and B) Dose response of the inhibition of complex I activities by rotenone (A) or piericidin A (B). Complex I activity was measured in cells by oxygen consumption using the polarography method (C and D) Rotenone, but not piericidin A, selectively decreases the survival of TH^+ neurons over $GABA^+$ neurons. Values represent means. Error bars indicate SEM. $n = 3$; *, $P < 0.05$; **, $P < 0.01$; ***, $P < 0.001$.

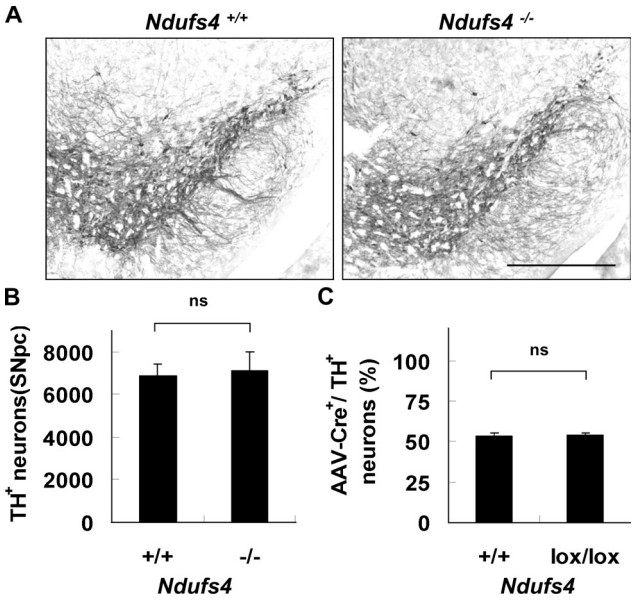

Figure 2. ***Ndufs4* inactivation does not cause dopamine neuron death.** (A) Representative photomicrographs of TH immunostaining of SNpc from 5-wk-old *Ndufs4*$^{+/+}$ and *Ndufs4*$^{-/-}$ mice. Bar, 500 µm. (B) Deletion of the *Ndufs4* gene does not decrease the total number of TH^+ neurons in the SNpc of 5-wk-old mice ($n = 5$ per group). (C) Inactivation of the *Ndufs4* gene in culture does not induce dopamine neuron death. E14 mesencephalic neurons were cultured from C57BL/6 or *Ndufs4*$^{lox/lox}$ mouse embryos. AAV1 viruses expressing Cre-GFP were added to the culture on DIV 4 to delete the *Ndufs4* gene in *Ndufs4*$^{lox/lox}$ cells. The number of TH^+ neurons was quantified 5 d after viral infection. Data are means ± SEM. $n = 3$.

subunits comprising mitochondrial complex I and is required for complete assembly and function of complex I (van den Heuvel et al., 1998; Budde et al., 2000; Petruzzella and Papa, 2002; Scacco et al., 2003; Vogel et al., 2007). We confirmed that deletion of the *Ndufs4* gene abolished complex I activity in midbrain mesencephalic neurons cultured from embryonic day (E) 14 mice (Choi et al., 2008). Surprisingly, dopamine neurons in *Ndufs4*$^{-/-}$ cultures appeared normal and survived as well as neurons from wild-type mice (Choi et al., 2008). The absence of complex I activity did not protect dopamine neurons against MPP^+ or rotenone toxicity as would be expected if these compounds act by inhibiting complex I, and *Ndufs4*$^{-/-}$ dopamine neurons were even more sensitive than *Ndufs4*$^{+/+}$ neurons to rotenone toxicity (Choi et al., 2008). These data question the long-held complex I inhibition hypothesis and suggest that there is a complex I–independent mechanism that renders dopamine neurons more susceptible than other neurons to rotenone and MPP^+. In this study, we provide further evidence to support our prior finding and elucidate complex I–independent mechanisms responsible for rotenone-induced dopamine neuron death.

Results

Complex I inhibition is insufficient to induce dopamine neuron death in culture and in the substantia nigra of *Ndufs4*$^{-/-}$ mice

We previously reported a lack of correlation between complex I inhibition and dopamine neuron death upon rotenone treatment or *Ndufs4* deletion (Choi et al., 2008). Piericidin A is another well-characterized mitochondrial complex I inhibitor (Gutman et al., 1970; Murai et al., 2006). It is at least as potent as rotenone in inhibiting complex I activity in primary mesencephalic cells ($IC_{50} = 20$ or 10 nM for rotenone or piericidin A, respectively; Fig. 1, A and B). We used antibodies against tyrosine hydroxylase (TH), the rate-limiting enzyme in dopamine biosynthesis, as a marker for dopamine neurons. Although 5 nM rotenone had very little effect on complex I activity, it selectively killed 50% of the TH^+ dopamine neurons (Fig. 1 C). In contrast, 20 nM piericidin A, which inhibited 65–70% of complex I activity, did not induce selective dopamine neuron death (Fig. 1 D).

We next quantified the number of TH^+ dopamine neurons in the SNpc of 5-wk-old *Ndufs4*$^{+/+}$ and *Ndufs4*$^{-/-}$ mice by stereological analysis. Although *Ndufs4*$^{-/-}$ mice die at postnatal week 7, they appear healthy until ∼5 wk of age (Kruse et al., 2008). The TH-staining pattern and cell distribution were comparable in both genotypes (Fig. 2 A). There was no difference in the total number of TH^+ dopamine neurons in the SNpc (Fig. 2 B). Similar results were obtained with 6–7-wk-old mice (Fig. S1). The number of $NeuN^+$ (neuronal nuclei) total neurons in the SNpc was also similar in both *Ndufs4*$^{+/+}$ and *Ndufs4*$^{-/-}$ mice (unpublished data).

One might argue that the *Ndufs4* deletion in *Ndufs4*$^{-/-}$ mice causes developmental compensation by other genes or other developmental defects that minimize the effect of complex I inhibition on dopamine neuron death. An in vitro gene knockout system was used to exclude this possibility. Primary mesencephalic neurons were cultured from wild-type or *Ndufs4*$^{lox/lox}$ embryos and infected with an adeno-associated virus (AAV) expressing Cre-GFP. Western analysis confirmed that AAV-Cre indeed knocked down Ndufs4 protein expression in *Ndufs4*$^{lox/lox}$

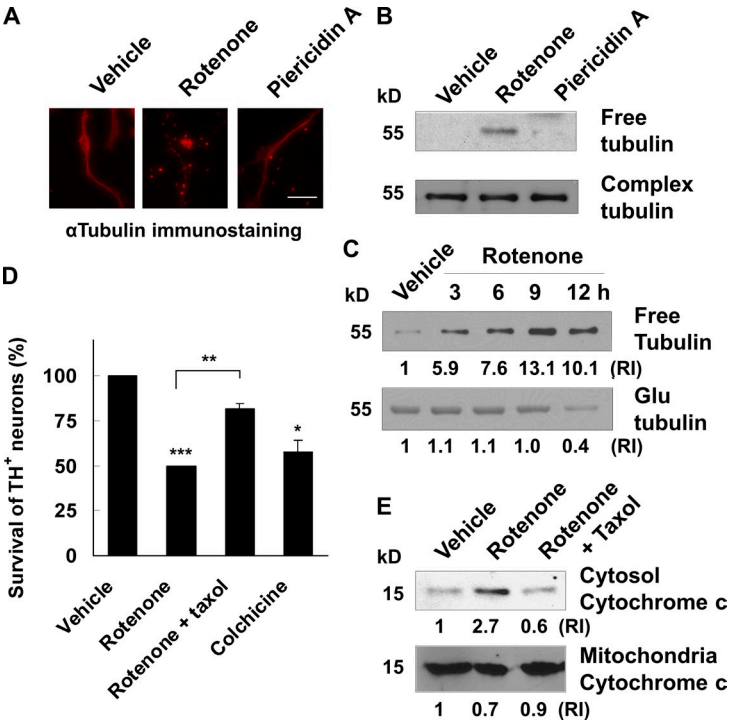

Figure 3. **Rotenone-induced dopamine neuron death is mediated through microtubule depolymerization.** E14 mouse mesencephalic neurons were treated on DIV 6 as indicated. (A) 5 nM rotenone, but not 10 nM piericidin A, induces microtubule fragmentation, which is indicative of microtubule depolymerization. Images are representative photomicrographs of immunostaining for α-tubulin 9 h after treatment. Bar, 30 µm. (B) Western blot analysis reveals an increase in free (depolymerized) tubulin after a 9-h treatment with 5 nM rotenone but not with 10 nM piericidin A. Complex (polymerized) tubulin was used as a control. (C) A time course of 10 nM rotenone–induced microtubule depolymerization was analyzed by Western blotting. Anti–α-tubulin antibody was used to detect free tubulin, whereas anti–Glu-tubulin antibody was used to detect the detyrosinated, relatively old or stable form of tubulin. (D) 10 nM taxol attenuates dopamine neuron death induced by 5 nM rotenone for 24 h, whereas 5 µM colchicine for 24 h kills dopamine neurons. (E) Cotreatment with 10 nM taxol blocks cytochrome *c* release induced by 5 nM rotenone for 9 h. The relative intensity (RI) of protein bands on Western blots was quantified using ImageJ. Data are means ± SEM. $n = 3$; *, $P < 0.05$; **, $P < 0.01$; ***, $P < 0.001$.

cultures (Fig. S2). For both cultures, ~50% of total TH$^+$ neurons were AAV1-Cre-GFP$^+$, indicating that Cre deletion of the *Ndufs4* gene in culture does not decrease dopamine neuron survival (Fig. 2 C). Together, these data further support our prior finding that complex I inhibition is insufficient to induce selective dopamine neuron death.

Rotenone-induced dopamine neuron death may involve microtubule depolymerization, accumulation of dopamine, and reactive oxygen species (ROS)

If rotenone is toxic for cultured dopamine neurons lacking complex I activity, what is the alternative mechanism for rotenone toxicity? It has been reported that rotenone induces microtubule depolymerization, which disrupts vesicular transport and causes dopamine accumulation and oxidative stress (Brinkley et al., 1974; Marshall and Himes, 1978; Ren et al., 2005). To evaluate microtubule depolymerization, we performed immunostaining for α-tubulin to visualize microtubules (Fig. 3 A) and Western blot analysis to detect free (depolymerized) versus complex (polymerized) tubulin (Fig. 3 B). Interestingly, rotenone, but not piericidin A, caused microtubule depolymerization in primary mesencephalic cultures, correlating with their selective toxicity to dopamine neurons. In addition, the level of free tubulin was increased 3–12 h after rotenone treatment (Fig. 3 C), whereas the detyrosinated, relatively "old" or stable form of tubulin (Glu-tubulin; Ertürk et al., 2007) was decreased 9–12 h after rotenone treatment (Fig. 3 C). Inhibiting microtubule depolymerization by cotreatment with taxol, a microtubule-stabilizing agent, attenuated rotenone-induced TH$^+$ neuron death as well as cytochrome *c* release (Fig. 3, D and E). Furthermore, treatment with colchicine, a known microtubule-depolymerizing agent, induced TH$^+$ neuron death to the same extent as rotenone (Fig. 3 D). These data implicate microtubule depolymerization as an initial cell death signal upstream from cytochrome *c* release and activation of the mitochondrial apoptotic pathway.

Treatment of cell cultures with rotenone or colchicine increased intracellular dopamine (Fig. 4 A). Rotenone-induced dopamine accumulation was blocked by cotreatment with taxol, linking microtubule depolymerization to dopamine accumulation. Rotenone-induced dopamine neuron death was attenuated by pretreatment with α-methyl-ρ-tyrosine, an inhibitor of dopamine biosynthesis (Fig. 4 B). α-Methyl-ρ-tyrosine also prevented rotenone-induced dopamine accumulation (Fig. 4 C). These data suggest that rotenone and colchicine increased intracellular dopamine to a toxic level, which contributes to their toxicity to dopamine neurons.

Consistent with dopamine accumulation, rotenone treatment increased intracellular ROS content (Fig. 5 A). Importantly, taxol attenuated rotenone induction of ROS. Finally, treatment with *N*-acetylcysteine, a free-radical scavenger and ROS inhibitor, protected TH$^+$ neurons from rotenone toxicity (Fig. 5 B). Collectively, these data suggest that the accumulation of dopamine and ROS acts downstream from rotenone-induced microtubule depolymerization and underlies rotenone toxicity to dopamine neurons.

Role of NADH, microtubule dysfunction, dopamine, and ROS in rotenone toxicity and the hypersensitivity of *Ndufs4*$^{-/-}$ dopamine neurons

To investigate the mechanism underlying the enhanced sensitivity of *Ndufs4*$^{-/-}$ dopamine neurons to rotenone, we cultured *Ndufs4*$^{+/+}$ and *Ndufs4*$^{-/-}$ neurons from mesencephalons of individual E14 embryos obtained by breeding *Ndufs4*$^{+/-}$ mice. As with wild-type cultures, piericidin A did not induce dopamine

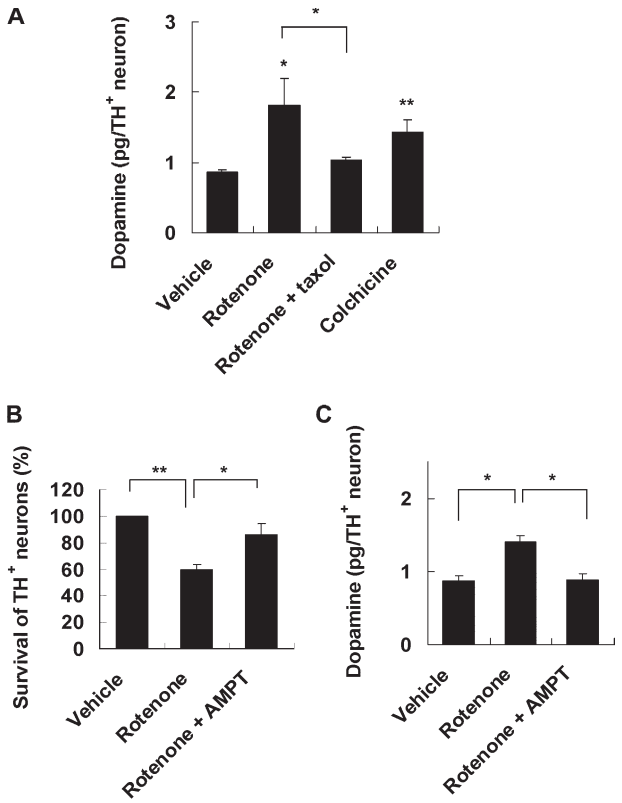

Figure 4. **Dopamine accumulation underlies rotenone toxicity.** (A) 10 nM rotenone for 8 h and 5 µM colchicine for 8 h increase total intracellular dopamine content, whereas cotreatment with 10 nM taxol blocks rotenone-induced dopamine accumulation. (B) Rotenone-induced dopamine neuron death is attenuated by pretreatment with α-methyl-ρ-tyrosine (AMPT), a dopamine synthesis inhibitor. 0.2-mM α-methyl-ρ-tyrosine was added 2 h before and maintained during 5 nM rotenone treatment for 24 h. (C) 0.2 mM α-methyl-ρ-tyrosine prevents 10 nM rotenone–induced dopamine accumulation. Data are means ± SEM. $n = 3$; *, $P < 0.05$; **, $P < 0.01$.

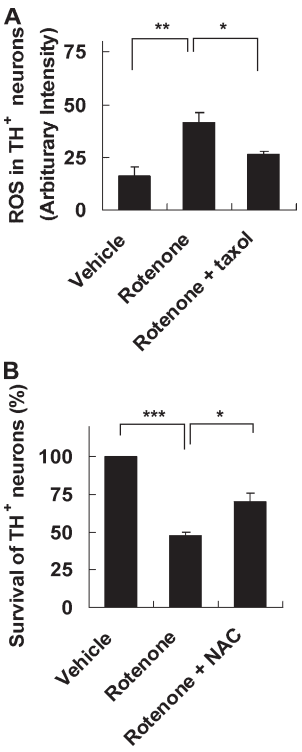

Figure 5. **Oxidative stress contributes to rotenone-induced dopamine neuron death.** (A) 5 nM rotenone for 12 h increases ROS production in TH+ neurons, which is prevented by cotreatment with 10 nM taxol. (B) Cotreatment with 0.5 mM *N*-acetylcysteine (NAC), an antioxidant, reduces 24-h 5-nM rotenone–induced TH+ neuron death. Data are means ± SEM. $n = 3$; *, $P < 0.05$; **, $P < 0.01$; ***, $P < 0.001$.

neuron death in *Ndufs4*$^{-/-}$ cultures (Fig. 6 A). Furthermore, rotenone caused microtubule depolymerization (Fig. 6 B), and either rotenone or colchicine induced dopamine neuron death (Fig. 6, C and D) in *Ndufs4*$^{-/-}$ cultures lacking complex I activity. These data suggest that microtubule depolymerization may be responsible for toxicity independent of complex I inhibition.

Significantly, *Ndufs4*$^{-/-}$ dopamine neurons were even more sensitive to either rotenone or colchicine (Fig. 6, C and D). These data suggest that although complex I inhibition by itself is insufficient to kill dopamine neurons, it can potentiate dopamine neuron toxicity induced by microtubule dysfunction. What mechanisms underlie this hypersensitivity? Because rotenone induced similar levels of microtubule depolymerization in both *Ndufs4*$^{+/+}$ and *Ndufs4*$^{-/-}$ cultures (Fig. 6 B), loss of complex I activity must act outside of microtubule stability to make dopamine neurons more vulnerable to microtubule dysfunction. We hypothesize that loss of complex I activity elevates the complex I substrate NADH, which stimulates endogenous dopamine biosynthesis by enhancing the recycling of tetrahydrobiopterin, a cofactor for TH (Vrecko et al., 1993, 1997). However, under resting conditions, the increase in dopamine may be modest and insufficient to cause oxidative stress because vesicular transport and release are sufficient to maintain low cytoplasmic dopamine concentrations. Upon rotenone treatment, the normal vesicular dopamine transport and release may be blocked as a result of microtubule destabilization. Thus, the combination of *Ndufs4* deletion and microtubule dysfunction causes more dopamine accumulation and ROS production than microtubule dysfunction alone, resulting in the hypersensitivity of *Ndufs4*$^{-/-}$ dopamine neurons to rotenone or colchicine.

To test this hypothesis, we measured NADH content in mesencephalic neurons cultured from *Ndufs4*$^{+/+}$ and *Ndufs4*$^{-/-}$ littermates by two-photon microscopy (Kuksa et al., 2003). Indeed, there was a statistically significant increase in NADH levels in cultures from *Ndufs4*$^{-/-}$ mice (Fig. 7 A). Rotenone treatment increased intracellular dopamine content in TH+ neurons from *Ndufs4*$^{+/+}$ cultures, and the increase was much greater in TH+ neurons prepared from *Ndufs4*$^{-/-}$ mice (Fig. 7 B). Cotreatment with taxol significantly blocked rotenone induction of dopamine accumulation in both cultures (Fig. 7 C). Furthermore, α-methyl-ρ-tyrosine improved the survival of TH+ neurons cultured from *Ndufs4*$^{-/-}$ mice to the same level as those from *Ndufs4*$^{+/+}$ mice.

Consistent with the dopamine increase, rotenone-induced ROS increase was greater in TH+ neurons prepared from *Ndufs4*$^{-/-}$ mice than in those from *Ndufs4*$^{+/+}$ mice (Fig. 8 A). Taxol attenuated rotenone induction of ROS to the same level in both cultures (Fig. 8 B). Finally, treatment with *N*-acetylcysteine protected TH+ neurons of both genotypes from rotenone toxicity to a similar degree (Fig. 8 C). Collectively,

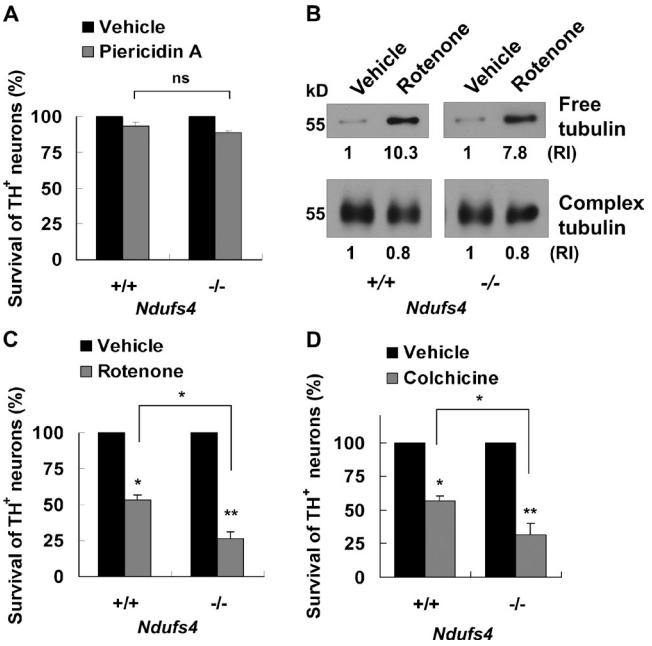

Figure 6. ***Ndufs4*-deficient dopamine neurons are more sensitive to rotenone and colchicine.** Mesencephalic neurons were cultured from individual E14 *Ndufs4*$^{+/+}$ and *Ndufs4*$^{-/-}$ embryos. (A) 10 nM piericidin A for 24 h does not cause dopamine neuron death in *Ndufs4*$^{+/+}$ or *Ndufs4*$^{-/-}$ cultures. (B) 5 nM rotenone for 9 h increases free (depolymerized) tubulin to the same extent in *Ndufs4*$^{-/-}$ cultures as it does in *Ndufs4*$^{+/+}$ cultures. The relative intensity (RI) of tubulin protein bands on Western blots was quantified using ImageJ. (C) 5 nM rotenone for 24 h kills more *Ndufs4*$^{-/-}$ dopamine neurons than *Ndufs4*$^{+/+}$ ones. (D) 5 µM colchicine for 24 h exerts more toxicity in dopamine neurons prepared from *Ndufs4*$^{-/-}$ than from *Ndufs4*$^{+/+}$ embryos. Data are means ± SEM. *n* = 3; *, P < 0.05; **, P < 0.01.

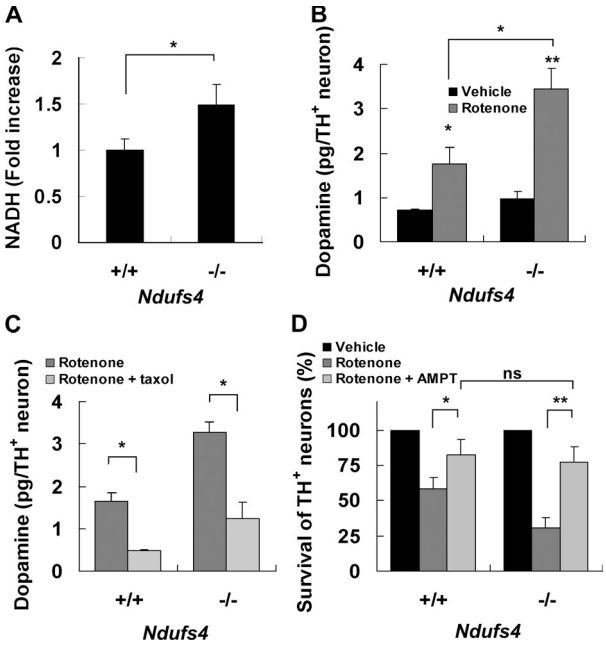

Figure 7. **NADH and dopamine accumulation underlie hypersensitivity of *Ndufs4*$^{-/-}$ neurons to rotenone.** Mesencephalic neurons were cultured from individual E14 *Ndufs4*$^{+/+}$ and *Ndufs4*$^{-/-}$ embryos. (A) Deletion of the *Ndufs4* gene increases basal intracellular NADH content. (B) 8-h 10-nM rotenone–induced intracellular dopamine accumulation is significantly higher in *Ndufs4*$^{-/-}$ cultures than in *Ndufs4*$^{+/+}$ cultures. (C) 10 nM taxol inhibits 8-h 10-nM rotenone–induced dopamine accumulation in both *Ndufs4*$^{+/+}$ and *Ndufs4*$^{-/-}$ cultures. (D) Pretreatment with 0.2-mM α-methyl-ρ-tyrosine (AMPT) protects dopamine neurons cultured from both *Ndufs4*$^{+/+}$ and *Ndufs4*$^{-/-}$ embryos against 5-nM rotenone toxicity for 24 h. Data are means ± SEM. *n* = 3–4; *, P < 0.05; **, P < 0.01.

these data suggest that the increase in basal NADH and the greater accumulation of dopamine and ROS after rotenone treatment in *Ndufs4*$^{-/-}$ cultures may explain why dopamine neurons lacking complex I activity are more sensitive to rotenone.

Rotenone toxicity to dopamine neurons may involve VMAT2 inhibition and the accumulation of cytoplasmic dopamine

Cytosolic, but not vesicular, dopamine is subject to oxidation, which promotes oxidative stress (Hastings et al., 1996). Thus, we determined whether rotenone increases cytosolic dopamine. Cultures treated with reserpine, an inhibitor of VMAT (vesicular monoamine transporter), were used as a positive control. As expected, reserpine increased cytosolic dopamine while decreasing vesicular dopamine (Fig. 9, A and B). Rotenone did not change the level of vesicular dopamine but significantly increased total (Fig. 4 A) as well as cytosolic (Fig. 9 B) dopamine. To further test this hypothesis, we enhanced VMAT2 function by transducing cultures with an adenovirus expressing VMAT2 (Mosharov et al., 2009); this treatment inhibited rotenone-induced TH$^+$ neuron death (Fig. 9 C). These data support the hypothesis that rotenone disrupts VMAT2 function and thereby enhances accumulation of cytoplasmic dopamine, which is toxic.

Discussion

Although mitochondrial complex I dysfunction has long been implicated in dopamine neuron death and the pathogenesis of Parkinson's disease, a causal relationship has not been firmly established. Dopamine neurons cultured for 1 wk from the mesencephalon of E14 *Ndufs4*$^{-/-}$ mouse embryos have no significant complex I activity, yet they appear normal without apparent defects in survival (Choi et al., 2008). The objective of this study was to provide additional evidence to support our prior finding that complex I inhibition is not sufficient to induce dopamine neuron death and to elucidate alternative mechanisms underlying rotenone-induced, complex I–independent dopamine neuron toxicity. We demonstrate in this study that piericidin A, another potent complex I inhibitor, does not induce selective dopamine neuron death, that in-culture deletion of the *Ndufs4* gene does not kill dopamine neurons, and that *Ndufs4* deletion does not change the number of TH$^+$ neurons in the SNpc in vivo in 5-wk-old mice. These data support our prior finding that complex I inhibition is not a direct cause of dopamine neuron death.

What is the mechanism by which rotenone selectively induces the death of dopamine neurons lacking complex I activity? We illustrate that rotenone causes microtubule depolymerization and the accumulation of dopamine and ROS in mesencephalic cultures.

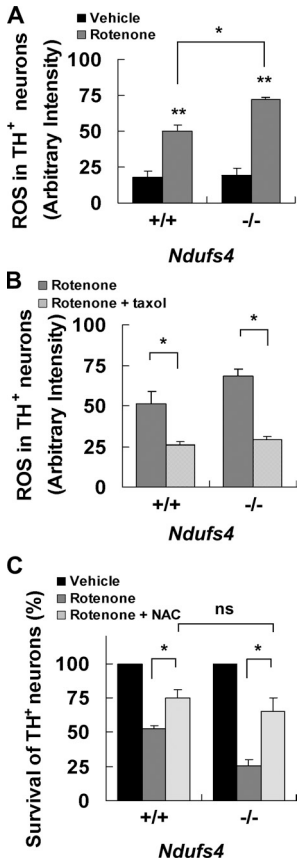

Figure 8. **Role of ROS production in the hypersensitivity of *Ndufs4*$^{-/-}$ neurons to rotenone.** Mesencephalic neurons were cultured from individual E14 *Ndufs4*$^{+/+}$ and *Ndufs4*$^{-/-}$ embryos. (A) 5 nM rotenone for 8 h increases intracellular ROS significantly more in dopamine neurons cultured from *Ndufs4*$^{-/-}$ embryos than those from *Ndufs4*$^{+/+}$ embryos. (B) 10 nM taxol prevents 8-h 5-nM rotenone–induced ROS production in *Ndufs4*$^{+/+}$ and *Ndufs4*$^{-/-}$ cultures. (C) 0.5 mM *N*-acetylcysteine (NAC) protects dopamine neurons cultured from both *Ndufs4*$^{+/+}$ and *Ndufs4*$^{-/-}$ embryos against 5-nM rotenone toxicity for 24 h. Data are means ± SEM. $n = 3–4$; *, $P < 0.05$; **, $P < 0.01$.

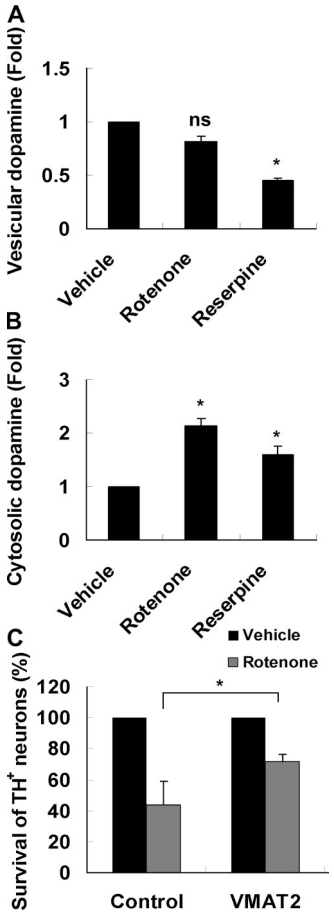

Figure 9. **Rotenone increases dopamine accumulation in the cytosol, suggesting that it may inhibit VMAT2 activity.** (A and B) E14 mouse mesencephalic cultures were treated with 10 nM rotenone for 8 h or 0.2 µM reserpine for 8 h. Dopamine concentration was measured from both synaptosome (vesicular; A) and cytosolic fractions (B). (C) Ectopic expression of VMAT2 protects dopamine neurons against rotenone. E14 mouse mesencephalic cultures were infected with VMAT2-expressing adenovirus or control GFP virus 2 d before 5-nM rotenone treatment for 24 h. The total number of TH+ neurons was counted. Data are means ± SEM. $n = 3$; *, $P < 0.05$.

Inhibition of microtubule depolymerization by cotreatment with taxol almost completely inhibited these processes and blocked rotenone-induced loss of TH+ neurons cultured from both *Ndufs4*$^{+/+}$ and *Ndufs4*$^{-/-}$ littermates. Furthermore, piericidin A did not cause microtubule depolymerization. Treatment with colchicine, a microtubule-depolymerizing agent, induced dopamine accumulation and dopamine neuron death. These data implicate microtubule depolymerization and the accumulation of dopamine and ROS as alternative mechanisms underlying rotenone-induced, complex I–independent dopamine neuron death. Our data are consistent with previous work from other laboratories (Ren et al., 2005; Feng, 2006; Ogburn and Figueiredo-Pereira, 2006).

We discovered that loss of complex I activity elevates baseline NADH levels. The NADH increase and microtubule destabilization associated with rotenone treatment cause greater dopamine and ROS accumulation in *Ndufs4*$^{-/-}$ dopamine neurons than in *Ndufs4*$^{+/+}$ dopamine neurons. This may explain why rotenone-induced TH+ neuron loss is greater in *Ndufs4*$^{-/-}$ neurons compared with *Ndufs4*$^{+/+}$ neurons. This hypothesis agrees with the report that overproduction of dopamine is sufficient to induce dopamine neuron death (Park et al., 2007b).

Interestingly, several Parkinson's disease–related genes, including *parkin* and *α-synuclein*, have been implicated in the regulation of microtubule dynamics. Overexpression of α-synuclein impairs microtubule-dependent trafficking (Lee et al., 2006). Parkin, a protein–ubiquitin E3 ligase, ubiquitinates α- and β-tubulin and accelerates their degradation (Ren et al., 2003). Parkinson's disease–linked mutations abolish these effects of parkin, which may result in the accumulation of misfolded or damaged tubulin. Parkin also protects dopamine neurons against colchicine (Ren et al., 2009). Transgenic mice expressing a mutant microtubule-associated protein tau found in frontotemporal dementia develop early onset tremor, bradykinesia, abnormal gait, and postural instability, which are reversible by L-3,4-dihydroxyphenylalanine (Ittner et al., 2008). Our data illustrate that treatment with the microtubule-depolymerizing agent colchicine is sufficient to cause dopamine neuron death in primary cultures. Together with our data on the differential effects of rotenone and piericidin A on microtubule function and dopamine neuron death, these results

suggest that damage and malfunction of microtubules may underlie dopamine neuron death in Parkinson's disease. Microtubule dysfunction could interfere with the axonal transport of essential molecules from the cell body to the axon terminals as well as removing molecules destined for degradation away from the axon. Thus, the microtubule dysfunction mechanism could explain, at least in part, the "dying back" phenomenon of dopamine neurons in Parkinson's disease, a process in which neurites degenerate before cell death.

Microtubule function is required for vesicular transport and release. Our data showed that rotenone-induced microtubule depolymerization led to an increase in total dopamine. However, only cytosolic, but not vesicular, dopamine is subject to oxidation, which elevates ROS and can cause neuron death (Hastings et al., 1996). Indeed, rotenone-induced increase in total dopamine was coupled with an increase in cytosolic dopamine. Because VMAT2 is the primary transporter that packages dopamine into presynaptic vesicles in dopamine neurons of the SNpc, our data implicate rotenone inhibition of VMAT2 function in primary dopamine neurons. The combined effect of microtubule depolymerization and VMAT2 inhibition increases total and cytosolic dopamine after rotenone treatment. Consistent with our findings, transgenic mice with low VMAT2 activity have reduced vesicular dopamine content and develop progressive dopamine neuron degeneration (Caudle et al., 2007). Rotenone inhibits and redistributes VMAT2 and increases cytosolic dopamine in SHSY5Y cells (Watabe and Nakaki, 2007, 2008).

Our results do not seem to agree with the findings derived from ectopic expression of *Ndi1*, a yeast single-subunit NADH dehydrogenase gene. Ectopic expression of *Ndi1* rescues dopamine neurons from rotenone toxicity in vitro and in vivo, leading to the conclusion that complex I inhibition is obligatory for dopamine neuron death in the rotenone model of Parkinson's disease (Sherer et al., 2003a, 2007; Marella et al., 2008). However, alternative explanations exist for these results. For example, per our hypothesis, ectopic overexpression of *Ndi1* could reduce NADH concentration and subsequent dopamine biosynthesis in dopamine neurons, making them less vulnerable to rotenone. Furthermore, because intracellular ATP and other NTPs can bind to cytochrome *c*, inhibit apoptosome formation, and are critical prosurvival factors (Chandra et al., 2006), it is conceivable that overexpressing *Ndi1* may increase ATP production and promote the survival of dopamine cells against a host of cell death signals that are unrelated to complex I inhibition, such as oxidative stress. Indeed, overexpression of *Ndi1* completely blocked cell death induced by several pesticides that are not known to be complex I inhibitors, including pyridaben, fenpyroximate, fenazaquin, and tebufenpyrad (Sherer et al., 2007). *Ndi1* expression also prevented cell death induced by paraquat (Park et al., 2007a), whose cytotoxicity is largely caused by oxidative stress but is independent of complex I inhibition (Day et al., 1999; Jones and Vale, 2000; Dauer and Przedborski, 2003; Bonneh-Barkay et al., 2005; McCormack et al., 2005; Richardson et al., 2005).

Intriguingly, *Ndufs4*$^{-/-}$ dopamine neurons were even more sensitive to rotenone or colchicine. The loss of complex I activity as a result of *Ndufs4* gene inactivation coupled with microtubule dysfunction exacerbated the accumulation of dopamine and ROS. These data suggest that although complex I inhibition is insufficient to kill dopamine neurons, it can potentiate dopamine neuron death caused by microtubule dysfunction. Our results suggest that the combination of inhibiting complex I and disrupting microtubule dynamics, either by genetic mutations or exposure to toxicants, may present an increased risk for Parkinson's disease.

Materials and methods

Generation of *Ndufs4*-null (*Ndufs4*$^{-/-}$) mice or embryos

The generation and characterization of *Ndufs4*$^{-/-}$ mice or embryos have been previously described (Kruse et al., 2008). The *Ndufs4* heterozygotes (*Ndufs4*$^{+/-}$) were bred to generate littermates of *Ndufs4*$^{+/+}$, *Ndufs4*$^{+/-}$, and *Ndufs4*$^{-/-}$ mice or embryos. PCR genotyping results were matched to each embryo at the end of the experiment. For the in vitro knockout experiments, mesencephalic primary neurons were cultured from E14 embryos taken from *Ndufs4*$^{lox/lox}$ mice (Kruse et al., 2008); embryos from wild-type C57BL/6 mice were used as controls.

Primary mesencephalic neuron cultures and drug treatments

Primary cultured dopamine neurons were prepared from E14 mouse embryos as previously described (Choi et al., 2008), either as single embryo cultures (for *Ndufs4*$^{+/+}$ and *Ndufs4*$^{-/-}$ cultures) or as pooled cultures from one to two pregnant C57BL/6 or *Ndufs4*$^{lox/lox}$ mice. The plug day was defined as E0.5. Drugs were obtained from Sigma-Aldrich unless otherwise specified. Drug treatments were performed in defined serum-free N2 medium (Invitrogen). Half of the media was replaced with N2 medium on the day before drug treatment and then again at the time of drug treatment. Cells treated with vehicle alone were used as controls. Cultures were treated on day in vitro (DIV) 5–6 with various drugs or on DIV 4 with AAV1-Cre-GFP. VMAT2-expressing adenovirus or control GFP virus (gift from E.V. Mosharov and D. Sulzer, Columbia University, New York, NY) was infected 2 d before rotenone treatment.

Polarography

Monitoring of mitochondrial oxygen consumption was performed in cells (not purified mitochondria) as previously described (Choi et al., 2008). In brief, healthy intact E14 cultured neurons grown on coverslips were placed in respiration buffer, pH 7.3, consisting of 225 mM mannitol, 75 mM sucrose, 10 mM KCl, 5 mM Hepes, 5 mM K_2HPO_4, and 1 mg/ml of freshly added defatted BSA in an oxygen-monitoring apparatus (5300A system; YSI Life Sciences) at 37°C. Mitochondrial complex I activity was measured by monitoring a 1.25-µM rotenone-sensitive oxygen consumption rate in the presence of complex I–specific substrates (10 mM pyruvate/2 mM malate/1 mM ADP). The amount of oxygen consumed was calculated, assuming the initial oxygen concentration in the buffer was 0.223 µmol O_2/ml.

Immunocytochemistry and quantification of TH$^+$ or γ-aminobutyric acid (GABA)–releasing neurons

These procedures were performed as previously described (Choi et al., 2008). In brief, cells were fixed with 4% paraformaldehyde/4% sucrose at room temperature for 30 min and blocked for 1 h in blocking buffer (PBS containing 5% BSA, 5% normal goat serum, and 0.1% Triton X-100). Cells were then incubated with primary antibodies in blocking buffer at 4°C overnight. Primary antibodies included mouse monoclonal antibody against TH (TH, 1:500; Sigma-Aldrich), rabbit polyclonal antibody against TH (1:50,000; Pel-Freez), rabbit polyclonal antibody against GABA (1:5,000; Sigma-Aldrich), and α-tubulin (1:2,000; Sigma-Aldrich). After three washes with PBS, cells were incubated at room temperature for 1 h with appropriate secondary antibodies. Secondary antibodies were Alexa Fluor 488 (or 568) goat anti–rabbit IgG and Alexa Fluor 568 (or 488) goat anti–mouse IgG (1:200; Invitrogen). Images for α-tubulin staining (Fig. 3 A) were taken at room temperature using an imaging system (Marianas; Intelligent Imaging Innovations, Inc.), which incorporates a fluorescence microscope (Axiovert 200M; Carl Zeiss, Inc.) with a motorized stage, a shuttered 175-W xenon lamp, a digital camera (CoolSNAP HQ; Roper Industries), and a 40× objective lens (Axiovert). Cells that were immunostained positive for TH or GABA antibodies and had neurites twice the length of the soma were scored as TH$^+$ or GABA$^+$ cells. All TH$^+$ cells on

a 9-mm diameter ACLAR embedding film were scored. The number of TH^+ neurons in one ACLAR embedding film was ~100–200 in control cultures (vehicle control). Cells that were immunostained positive for the GABA antibody were counted from five representative fields from each ACLAR embedding film and scored as the GABAergic population.

Immunohistochemistry and quantification of TH^+ neurons in the SNpc

5-wk-old *Ndufs4*$^{+/+}$ and *Ndufs4*$^{-/-}$ littermate mice were perfused with heparinized saline followed by 4% paraformaldehyde as previously described (Choi et al., 2010). Harvested brains were postfixed in 4% paraformaldehyde overnight and then cryoprotected in PBS with 30% sucrose for ≥2 d. Fixed brains were cut into 40-µm sections and collected in cryoprotectant. Sections were incubated with an antibody against TH (1:5,000; Pel-Freez) in PBS containing 0.1% Triton X-100, 5% BSA, and 5% goat serum. Sections were washed and incubated with biotin-labeled secondary antibody and avidin-biotin solution using the VECTASTAIN Elite kit (Vector Laboratories) for 1 h each at room temperature. Sections were developed in DAB for 2–5 min, rinsed several times in tap water, and mounted. Images for TH staining (Fig. 2 A) were collected at room temperature with an inverted fluorescence microscope (E400; Nikon) using a 4× objective lens (Nikon) equipped with a digital microscope camera (MagnaFire; Optronics, Inc.). MagnaFire software was used for system control and image processing. TH^+ neurons were counted stereologically as previously described (Mandir et al., 1999). In brief, low magnification (2.5×) images were taken under a microscope (Axiovert 200M) equipped with motorized stage in three axes. The boundaries of SNpc were outlined using the set of anatomical landmarks according to the mouse brain atlas (Hof et al., 2000). The number of TH^+ neurons was counted at high power (65×) at automatically selected random fields of the SNpc, and the number of total TH^+ neurons on each slide was calculated following optical dissector rules using a cell counter (StereoInvestigator System; MicroBrightField, Inc.). We began cell counting at the first slide of the SNpc section when TH^+ neurons were visible and then on every fourth slide through the entire SNpc. The estimate of the total number of TH^+ neurons in each brain was calculated using the optical dissector method (Mandir et al., 1999). Five brains from each genotype (*Ndufs4*$^{+/+}$ and *Ndufs4*$^{-/-}$) were analyzed for stereological cell counting and presented as the total number of TH^+ neurons in the SNpc of each brain.

Immunoblot analysis

Protein lysates were prepared from cells and analyzed by SDS-PAGE gel electrophoresis and Western blotting as previously described (Choi et al., 2010). Mouse monoclonal anti–cytochrome *c* antibody (1:3,000) was purchased from Santa Cruz Biotechnology, Inc. Antibodies against α-tubulin and Glu-tubulin were purchased from Sigma-Aldrich.

Preparation of the cytosolic and mitochondrial fraction for cytochrome *c* release assay

Cytochrome *c* release was assayed as previously described (Gross et al., 1998; Choi et al., 2004). In brief, cells were washed with PBS, resuspended in isotonic buffer A (250 mM sucrose, 1 mM EGTA, 10 mM Hepes, pH 8.0, 1 mM DTT, and protease inhibitors), and homogenized using an A-type Dounce homogenizer (Kontes) 40 times. Nuclei and unbroken cells were removed by centrifugation at 120 *g* for 5 min as the pellet. The supernatant was centrifuged again at 10,000 *g* for 10 min to collect the heavy membrane pellet (mitochondria), whereas the supernatant was designated the cytosolic fraction (cytosol). The heavy membrane pellet was lysed by vortexing and resuspending it in resuspension buffer (10 mM Hepes, 5 mM $MgCl_2$, 42 mM KCl, and 1% Triton X-100) for 5 min on ice.

Preparation of free and complex tubulin

Free or polymerized tubulin was extracted from cultured cells as previously described (Jiang et al., 2006). In brief, midbrain neuronal cultures maintained in 24-well plates were washed twice at 37°C with 1 ml of buffer A containing 0.1 M MES, pH 6.75, 1 mM $MgSO_4$, 2 mM EGTA, 0.1 mM EDTA, and 4 M glycerol. The cultures were then incubated at 37°C for 5 min in 300 µl of free tubulin extraction buffer (buffer A plus 0.1% [vol/vol] Triton X-100 and protease inhibitors). The extracts were centrifuged at 37°C for 2 min at 16,000 *g*. The supernatant fractions contained free cytosolic tubulin. The pellet fraction and lysed cells remaining in the culture dish retained polymerized tubulin in microtubules and were dissolved in 600 µl of 25 mM Tris, pH 6.8, plus 0.5% SDS. Equal amounts of total protein from free or polymerized tubulin fractions were analyzed by Western blotting with an anti–α-tubulin antibody.

ROS labeling and quantification

Cells were incubated at 37°C for 15 min with 5 µM CM-DCFDA (5-(and-6)-chloromethyl-2′,7′-dichlorodihydrofluorescein diacetate acetyl ester; Invitrogen) and washed with and then incubated in PBS at 37°C for another 15 min. The images of eight fields from each well were captured with an inverted fluorescence microscope (E400) equipped with a digital camera (MagnaFire) and a temperature-controlled stage at 37°C. Cells were then fixed with 4% paraformaldehyde and processed for anti-TH immunostaining. After staining, images from the same eight fields were captured and compared. The staining intensity of the CM-DCFDA dye (ROS) in the TH^+ neuron population was quantified using the ImageJ program (National Institutes of Health). All TH^+ neurons in captured images were scored, and the mean ROS level per TH^+ neuron was calculated.

Measurement of intracellular NADH content

Two-photon excitation microscopy was used to measure the intracellular NADH content as previously described (Kuksa et al., 2003). Cells were grown for 5 d on 25-mm glass coverslips (Corning). The coverslips were mounted on a temperature-controlled microscopic stage (Heating Insert P; Carl Zeiss, Inc.) installed on the microscope to maintain the medium temperature at 37°C. The objective lens was preheated up to 37°C by an air stream incubator (ASI 400; Nevtek). NADH autofluorescence (435–485 nm) from the sample was collected through the objective lens, separated from the excitation light by a dichroic mirror, filtered by BG39 to remove scattered UV light, and directed to a photomultiplier tube detector (LSM 510; Carl Zeiss, Inc.). NADH intensity was imaged using a 20× 1.3 NA Plan Neofluar objective lens (Carl Zeiss, Inc.) and 76-MHz, 100-fs pulses of a 730-nm light from a mode-locked Ti:Sapphire laser (Mira; Coherent, Inc.). Images were analyzed with the AIM Image Examiner program (Carl Zeiss, Inc.) and the ImageJ program.

Dopamine measurement

E14 mesencephalic primary neurons (3–4 × 10^5 cells) were plated on each well of the 24-well plates. Duplicate sets of cells were treated equally with drugs or vehicle control. One set was fixed and immunostained for TH to quantify the total number of TH^+ neurons. The other set (2–4 wells for each treatment) of cells was frozen on dry ice, stored at −80°C, and sent to the Neurochemistry Core Laboratory at Vanderbilt University's Center for Molecular Neuroscience Research to analyze for dopamine content, which was done without prior knowledge of genotypes or drug treatments. In brief, cells were homogenized with 0.1 M trichloroacetic acid containing 10 mM sodium acetate/0.1 mM EDTA/1 mM isoproterenol (internal standard)/10.5% methanol, pH 3.8, and centrifuged at 10,000 *g* for 20 min. Total dopamine content in the supernatant was quantified by HPLC coupled with electrochemical detection (0.7 V). The HPLC system (Antec Leyden) consisted of a 515 HPLC pump, a 717 plus autosampler, an electrochemical detector (Decade II; Antec Leyden), and an HPLC column (150 × 4.6 mm; Nucleosil C18; Phenomenex). The homogenization buffer was used as the mobile phase (0.7 ml/min), and 20 µl of the sample was injected onto an HPLC column (3.9 × 300 mm; Nova-Pak C18; Waters). Dopamine content was normalized to the number of TH^+ neurons in each treatment group. For the cytosolic or vesicular dopamine measurement, synaptosome and cytosol fractions were prepared using a synaptic vesicle preparation kit (SV0100; Sigma-Aldrich) and sent to the Neurochemistry Core Laboratory for dopamine measurement.

Statistical analysis

Data were from at least three independent experiments, each with at least duplicate or triplicate determinations. Statistical analyses of data were performed using two-way analysis of variance and posthoc Student's *t* test.

Online supplemental material

Fig. S1 shows the quantification of TH immunostaining of SNpc from 6–7-wk-old *Ndufs4*$^{+/+}$ and *Ndufs4*$^{-/-}$ mouse brains. Fig. S2 shows that AAV-Cre knocks down Ndufs4 protein expression in *Ndufs4*$^{lox/lox}$ cultures prepared from E14 mesencephalon. Online supplemental material is available at http://www.jcb.org/cgi/content/full/jcb.201009132/DC1.

We thank Dr. Eugene V. Mosharov (Columbia University) for the adenovirus expressing VMAT2 and Dr. Linda Wordeman for scientific discussions.

This work was supported by grants ES012215 and ES013696 from the National Institutes of Health (Z. Xia) and the Postdoctoral Fellowship Program of the Korea Science and Engineering Foundation (W.-S. Choi) and facilitated by grant P30 HD02274 from the National Institute of Child Health and Human Development and by grant NIEHS P30ES07033 from the University of Washington National Institute of Environmental Health Sciences–sponsored Center for Ecogenetics and Environmental Health.

Submitted: 28 September 2010
Accepted: 2 February 2011

References

Abou-Sleiman, P.M., M.M. Muqit, and N.W. Wood. 2006. Expanding insights of mitochondrial dysfunction in Parkinson's disease. *Nat. Rev. Neurosci.* 7:207–219. doi:10.1038/nrn1868

Betarbet, R., T.B. Sherer, G. MacKenzie, M. Garcia-Osuna, A.V. Panov, and J.T. Greenamyre. 2000. Chronic systemic pesticide exposure reproduces features of Parkinson's disease. *Nat. Neurosci.* 3:1301–1306. doi:10.1038/81834

Bonneh-Barkay, D., S.H. Reaney, W.J. Langston, and D.A. Di Monte. 2005. Redox cycling of the herbicide paraquat in microglial cultures. *Brain Res. Mol. Brain Res.* 134:52–56. doi:10.1016/j.molbrainres.2004.11.005

Brinkley, B.R., S.S. Barham, S.C. Barranco, and G.M. Fuller. 1974. Rotenone inhibition of spindle microtubule assembly in mammalian cells. *Exp. Cell Res.* 85:41–46. doi:10.1016/0014-4827(74)90210-9

Budde, S.M., L.P. van den Heuvel, A.J. Janssen, R.J. Smeets, C.A. Buskens, L. DeMeirleir, R. Van Coster, M. Baethmann, T. Voit, J.M. Trijbels, and J.A. Smeitink. 2000. Combined enzymatic complex I and III deficiency associated with mutations in the nuclear encoded NDUFS4 gene. *Biochem. Biophys. Res. Commun.* 275:63–68. doi:10.1006/bbrc.2000.3257

Caudle, W.M., J.R. Richardson, M.Z. Wang, T.N. Taylor, T.S. Guillot, A.L. McCormack, R.E. Colebrooke, D.A. Di Monte, P.C. Emson, and G.W. Miller. 2007. Reduced vesicular storage of dopamine causes progressive nigrostriatal neurodegeneration. *J. Neurosci.* 27:8138–8148. doi:10.1523/JNEUROSCI.0319-07.2007

Chandra, D., S.B. Bratton, M.D. Person, Y. Tian, A.G. Martin, M. Ayres, H.O. Fearnhead, V. Gandhi, and D.G. Tang. 2006. Intracellular nucleotides act as critical prosurvival factors by binding to cytochrome C and inhibiting apoptosome. *Cell*. 125:1333–1346. doi:10.1016/j.cell.2006.05.026

Choi, W.S., D.S. Eom, B.S. Han, W.K. Kim, B.H. Han, E.J. Choi, T.H. Oh, G.J. Markelonis, J.W. Cho, and Y.J. Oh. 2004. Phosphorylation of p38 MAPK induced by oxidative stress is linked to activation of both caspase-8- and -9-mediated apoptotic pathways in dopaminergic neurons. *J. Biol. Chem.* 279:20451–20460. doi:10.1074/jbc.M311164200

Choi, W.S., S.E. Kruse, R.D. Palmiter, and Z. Xia. 2008. Mitochondrial complex I inhibition is not required for dopaminergic neuron death induced by rotenone, MPP+, or paraquat. *Proc. Natl. Acad. Sci. USA*. 105:15136–15141. doi:10.1073/pnas.0807581105

Choi, W.S., G. Abel, H. Klintworth, R.A. Flavell, and Z. Xia. 2010. JNK3 mediates paraquat- and rotenone-induced dopaminergic neuron death. *J. Neuropathol. Exp. Neurol.* 69:511–520. doi:10.1097/NEN.0b013e3181db8100

Dauer, W., and S. Przedborski. 2003. Parkinson's disease: mechanisms and models. *Neuron*. 39:889–909. doi:10.1016/S0896-6273(03)00568-3

Day, B.J., M. Patel, L. Calavetta, L.Y. Chang, and J.S. Stamler. 1999. A mechanism of paraquat toxicity involving nitric oxide synthase. *Proc. Natl. Acad. Sci. USA*. 96:12760–12765. doi:10.1073/pnas.96.22.12760

Ertürk, A., F. Hellal, J. Enes, and F. Bradke. 2007. Disorganized microtubules underlie the formation of retraction bulbs and the failure of axonal regeneration. *J. Neurosci.* 27:9169–9180. doi:10.1523/JNEUROSCI.0612-07.2007

Feng, J. 2006. Microtubule: a common target for parkin and Parkinson's disease toxins. *Neuroscientist*. 12:469–476. doi:10.1177/1073858406293853

Gross, A., J. Jockel, M.C. Wei, and S.J. Korsmeyer. 1998. Enforced dimerization of BAX results in its translocation, mitochondrial dysfunction and apoptosis. *EMBO J.* 17:3878–3885. doi:10.1093/emboj/17.14.3878

Gutman, M., T.P. Singer, H. Beinert, and J.E. Casida. 1970. Reaction sites of rotenone, piericidin A, and amytal in relation to the nonheme iron components of NADH dehydrogenase. *Proc. Natl. Acad. Sci. USA*. 65:763–770. doi:10.1073/pnas.65.3.763

Hastings, T.G., D.A. Lewis, and M.J. Zigmond. 1996. Role of oxidation in the neurotoxic effects of intrastriatal dopamine injections. *Proc. Natl. Acad. Sci. USA*. 93:1956–1961. doi:10.1073/pnas.93.5.1956

Hof, P.R., W.G. Young, F.E. Bloom, P.V. Belichenko, and M.R. Celio, editors. 2000. Comparative Cytoarchitectonic Atlas of the C57BL/6 and 129/Sv Mouse Brains. Elsevier, Amsterdam. 284 pp.

Inden, M., Y. Kitamura, H. Takeuchi, T. Yanagida, K. Takata, Y. Kobayashi, T. Taniguchi, K. Yoshimoto, M. Kaneko, Y. Okuma, et al. 2007. Neurodegeneration of mouse nigrostriatal dopaminergic system induced by repeated oral administration of rotenone is prevented by 4-phenylbutyrate, a chemical chaperone. *J. Neurochem.* 101:1491–1504. doi:10.1111/j.1471-4159.2006.04440.x

Ittner, L.M., T. Fath, Y.D. Ke, M. Bi, J. van Eersel, K.M. Li, P. Gunning, and J. Götz. 2008. Parkinsonism and impaired axonal transport in a mouse model of frontotemporal dementia. *Proc. Natl. Acad. Sci. USA*. 105:15997–16002. doi:10.1073/pnas.0808084105

Jiang, Q., Z. Yan, and J. Feng. 2006. Neurotrophic factors stabilize microtubules and protect against rotenone toxicity on dopaminergic neurons. *J. Biol. Chem.* 281:29391–29400. doi:10.1074/jbc.M602740200

Jones, G.M., and J.A. Vale. 2000. Mechanisms of toxicity, clinical features, and management of diquat poisoning: a review. *J. Toxicol. Clin. Toxicol.* 38:123–128. doi:10.1081/CLT-100100926

Keeney, P.M., J. Xie, R.A. Capaldi, and J.P. Bennett Jr. 2006. Parkinson's disease brain mitochondrial complex I has oxidatively damaged subunits and is functionally impaired and misassembled. *J. Neurosci.* 26:5256–5264. doi:10.1523/JNEUROSCI.0984-06.2006

Kruse, S.E., W.C. Watt, D.J. Marcinek, R.P. Kapur, K.A. Schenkman, and R.D. Palmiter. 2008. Mice with mitochondrial complex I deficiency develop a fatal encephalomyopathy. *Cell Metab.* 7:312–320. doi:10.1016/j.cmet.2008.02.004

Kuksa, V., Y. Imanishi, M. Batten, K. Palczewski, and A.R. Moise. 2003. Retinoid cycle in the vertebrate retina: experimental approaches and mechanisms of isomerization. *Vision Res.* 43:2959–2981. doi:10.1016/S0042-6989(03)00482-6

Langston, J.W., P. Ballard, J.W. Tetrud, and I. Irwin. 1983. Chronic Parkinsonism in humans due to a product of meperidine-analog synthesis. *Science*. 219:979–980. doi:10.1126/science.6823561

Lee, H.J., F. Khoshaghideh, S. Lee, and S.J. Lee. 2006. Impairment of microtubule-dependent trafficking by overexpression of alpha-synuclein. *Eur. J. Neurosci.* 24:3153–3162. doi:10.1111/j.1460-9568.2006.05210.x

Mandir, A.S., S. Przedborski, V. Jackson-Lewis, Z.Q. Wang, C.M. Simbulan-Rosenthal, M.E. Smulson, B.E. Hoffman, D.B. Guastella, V.L. Dawson, and T.M. Dawson. 1999. Poly(ADP-ribose) polymerase activation mediates 1-methyl-4-phenyl-1, 2,3,6-tetrahydropyridine (MPTP)-induced parkinsonism. *Proc. Natl. Acad. Sci. USA*. 96:5774–5779. doi:10.1073/pnas.96.10.5774

Marella, M., B.B. Seo, E. Nakamaru-Ogiso, J.T. Greenamyre, A. Matsuno-Yagi, and T. Yagi. 2008. Protection by the NDI1 gene against neurodegeneration in a rotenone rat model of Parkinson's disease. *PLoS ONE*. 3:e1433. doi:10.1371/journal.pone.0001433

Marshall, L.E., and R.H. Himes. 1978. Rotenone inhibition of tubulin self-assembly. *Biochim. Biophys. Acta*. 543:590–594.

McCormack, A.L., J.G. Atienza, L.C. Johnston, J.K. Andersen, S. Vu, and D.A. Di Monte. 2005. Role of oxidative stress in paraquat-induced dopaminergic cell degeneration. *J. Neurochem.* 93:1030–1037. doi:10.1111/j.1471-4159.2005.03088.x

Mizuno, Y., S. Ohta, M. Tanaka, S. Takamiya, K. Suzuki, T. Sato, H. Oya, T. Ozawa, and Y. Kagawa. 1989. Deficiencies in complex I subunits of the respiratory chain in Parkinson's disease. *Biochem. Biophys. Res. Commun.* 163:1450–1455. doi:10.1016/0006-291X(89)91141-8

Mosharov, E.V., K.E. Larsen, E. Kanter, K.A. Phillips, K. Wilson, Y. Schmitz, D.E. Krantz, K. Kobayashi, R.H. Edwards, and D. Sulzer. 2009. Interplay between cytosolic dopamine, calcium, and alpha-synuclein causes selective death of substantia nigra neurons. *Neuron*. 62:218–229. doi:10.1016/j.neuron.2009.01.033

Murai, M., N. Ichimaru, M. Abe, T. Nishioka, and H. Miyoshi. 2006. Mode of inhibitory action of Deltalac-acetogenins, a new class of inhibitors of bovine heart mitochondrial complex I. *Biochemistry*. 45:9778–9787. doi:10.1021/bi060713f

Ogburn, K.D., and M.E. Figueiredo-Pereira. 2006. Cytoskeleton/endoplasmic reticulum collapse induced by prostaglandin J2 parallels centrosomal deposition of ubiquitinated protein aggregates. *J. Biol. Chem.* 281:23274–23284. doi:10.1074/jbc.M600635200

Pan-Montojo, F., O. Anichtchik, Y. Dening, L. Knels, S. Pursche, R. Jung, S. Jackson, G. Gille, M.G. Spillantini, H. Reichmann, and R.H. Funk. 2010. Progression of Parkinson's disease pathology is reproduced by intragastric administration of rotenone in mice. *PLoS ONE*. 5:e8762. doi:10.1371/journal.pone.0008762

Park, J.S., Y.F. Li, and Y. Bai. 2007a. Yeast NDI1 improves oxidative phosphorylation capacity and increases protection against oxidative stress and cell death in cells carrying a Leber's hereditary optic neuropathy mutation. *Biochim. Biophys. Acta*. 1772:533–542.

Park, S.S., E.M. Schulz, and D. Lee. 2007b. Disruption of dopamine homeostasis underlies selective neurodegeneration mediated by alpha-synuclein. *Eur. J. Neurosci.* 26:3104–3112. doi:10.1111/j.1460-9568.2007.05929.x

Parker, W.D. Jr., S.J. Boyson, and J.K. Parks. 1989. Abnormalities of the electron transport chain in idiopathic Parkinson's disease. *Ann. Neurol.* 26:719–723. doi:10.1002/ana.410260606

Petruzzella, V., and S. Papa. 2002. Mutations in human nuclear genes encoding for subunits of mitochondrial respiratory complex I: the NDUFS4 gene. *Gene*. 286:149–154. doi:10.1016/S0378-1119(01)00810-1

Ren, Y., J. Zhao, and J. Feng. 2003. Parkin binds to alpha/beta tubulin and increases their ubiquitination and degradation. *J. Neurosci.* 23:3316–3324.

Ren, Y., W. Liu, H. Jiang, Q. Jiang, and J. Feng. 2005. Selective vulnerability of dopaminergic neurons to microtubule depolymerization. *J. Biol. Chem.* 280:34105–34112. doi:10.1074/jbc.M503483200

Ren, Y., H. Jiang, F. Yang, K. Nakaso, and J. Feng. 2009. Parkin protects dopaminergic neurons against microtubule-depolymerizing toxins by attenuating microtubule-associated protein kinase activation. *J. Biol. Chem.* 284:4009–4017. doi:10.1074/jbc.M806245200

Richardson, J.R., Y. Quan, T.B. Sherer, J.T. Greenamyre, and G.W. Miller. 2005. Paraquat neurotoxicity is distinct from that of MPTP and rotenone. *Toxicol. Sci.* 88:193–201. doi:10.1093/toxsci/kfi304

Richardson, J.R., W.M. Caudle, T.S. Guillot, J.L. Watson, E. Nakamaru-Ogiso, B.B. Seo, T.B. Sherer, J.T. Greenamyre, T. Yagi, A. Matsuno-Yagi, and G.W. Miller. 2007. Obligatory role for complex I inhibition in the dopaminergic neurotoxicity of 1-methyl-4-phenyl-1,2,3,6-tetrahydropyridine (MPTP). *Toxicol. Sci.* 95:196–204. doi:10.1093/toxsci/kfl133

Scacco, S., V. Petruzzella, S. Budde, R. Vergari, R. Tamborra, D. Panelli, L.P. van den Heuvel, J.A. Smeitink, and S. Papa. 2003. Pathological mutations of the human NDUFS4 gene of the 18-kDa (AQDQ) subunit of complex I affect the expression of the protein and the assembly and function of the complex. *J. Biol. Chem.* 278:44161–44167. doi:10.1074/jbc.M307615200

Schapira, A.H., J.M. Cooper, D. Dexter, P. Jenner, J.B. Clark, and C.D. Marsden. 1989. Mitochondrial complex I deficiency in Parkinson's disease. *Lancet*. 333:1269. doi:10.1016/S0140-6736(89)92366-0

Seo, B.B., E. Nakamaru-Ogiso, T.R. Flotte, A. Matsuno-Yagi, and T. Yagi. 2006. In vivo complementation of complex I by the yeast Ndi1 enzyme. Possible application for treatment of Parkinson disease. *J. Biol. Chem.* 281:14250–14255. doi:10.1074/jbc.M600922200

Sherer, T.B., R. Betarbet, C.M. Testa, B.B. Seo, J.R. Richardson, J.H. Kim, G.W. Miller, T. Yagi, A. Matsuno-Yagi, and J.T. Greenamyre. 2003a. Mechanism of toxicity in rotenone models of Parkinson's disease. *J. Neurosci.* 23:10756–10764.

Sherer, T.B., J.H. Kim, R. Betarbet, and J.T. Greenamyre. 2003b. Subcutaneous rotenone exposure causes highly selective dopaminergic degeneration and alpha-synuclein aggregation. *Exp. Neurol.* 179:9–16. doi:10.1006/exnr.2002.8072

Sherer, T.B., J.R. Richardson, C.M. Testa, B.B. Seo, A.V. Panov, T. Yagi, A. Matsuno-Yagi, G.W. Miller, and J.T. Greenamyre. 2007. Mechanism of toxicity of pesticides acting at complex I: relevance to environmental etiologies of Parkinson's disease. *J. Neurochem.* 100:1469–1479.

van den Heuvel, L., W. Ruitenbeek, R. Smeets, Z. Gelman-Kohan, O. Elpeleg, J. Loeffen, F. Trijbels, E. Mariman, D. de Bruijn, and J. Smeitink. 1998. Demonstration of a new pathogenic mutation in human complex I deficiency: a 5-bp duplication in the nuclear gene encoding the 18-kD (AQDQ) subunit. *Am. J. Hum. Genet.* 62:262–268. doi:10.1086/301716

Vogel, R.O., M.A. van den Brand, R.J. Rodenburg, L.P. van den Heuvel, M. Tsuneoka, J.A. Smeitink, and L.G. Nijtmans. 2007. Investigation of the complex I assembly chaperones B17.2L and NDUFAF1 in a cohort of CI deficient patients. *Mol. Genet. Metab.* 91:176–182. doi:10.1016/j.ymgme.2007.02.007

Vrecko, K., J.G. Birkmayer, and J. Krainz. 1993. Stimulation of dopamine biosynthesis in cultured PC 12 phaeochromocytoma cells by the coenzyme nicotinamide adeninedinucleotide (NADH). *J. Neural Transm. Park. Dis. Dement. Sect.* 5:147–156. doi:10.1007/BF02251205

Vrecko, K., D. Storga, J.G. Birkmayer, R. Möller, E. Tafeit, R. Horejsi, and G. Reibnegger. 1997. NADH stimulates endogenous dopamine biosynthesis by enhancing the recycling of tetrahydrobiopterin in rat phaeochromocytoma cells. *Biochim. Biophys. Acta*. 1361:59–65.

Watabe, M., and T. Nakaki. 2007. Mitochondrial complex I inhibitor rotenone-elicited dopamine redistribution from vesicles to cytosol in human dopaminergic SH-SY5Y cells. *J. Pharmacol. Exp. Ther.* 323:499–507. doi:10.1124/jpet.107.127597

Watabe, M., and T. Nakaki. 2008. Mitochondrial complex I inhibitor rotenone inhibits and redistributes vesicular monoamine transporter 2 via nitration in human dopaminergic SH-SY5Y cells. *Mol. Pharmacol.* 74:933–940. doi:10.1124/mol.108.048546